Inorganic Chemistry

Article

pubs.acs.org/IC

A Donor–Acceptor Tetrathiafulvalene Ligand Complexed to Iron(II): Synthesis, Electrochemistry, and Spectroscopy of $[Fe(phen)_2(TTF\text{-}dppz)](PF_6)_2$

Nathalie Dupont,[†] Ying-Fen Ran,[‡] Shi-Xia Liu,*[,‡] Jakob Grilj,[†] Eric Vauthey,[†] Silvio Decurtins,[‡] and Andreas Hauser*[,†]

[†]Département de Chimie Physique, Université de Genève, 30 Quai Ernest-Ansermet, CH-1211 Genève 4, Switzerland

[‡]Departement für Chemie und Biochemie, Universität Bern, Freiestrasse 3, CH-3012 Bern, Switzerland

ABSTRACT: The synthesis and photophysical properties of the complex $[Fe(phen)_2(TTF\text{-}dppz)]^{2+}$ (TTF-dppz = 4′,5′-bis-(propylthio)tetrathiafulvenyl[*i*]dipyrido[3,2-*a*:2′,3′-*c*]-phenazine, phen = 1,10-phenanthroline) are described. In this complex, excitation into the metal–ligand charge transfer bands results in the population of a high-spin state of iron(II), with a decay lifetime of approximately 1.5 ns, in dichloromethane, at room temperature. An intraligand charge transfer state can also be obtained and has a lifetime of 38 ps. A mechanism for the different states reached is proposed based on transient absorption spectroscopy.

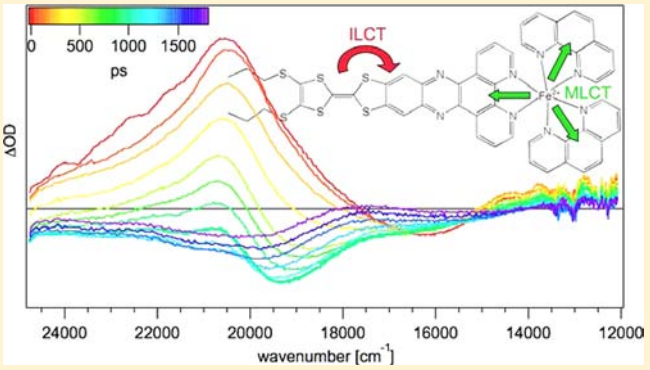

1. INTRODUCTION

Light-induced processes in spin-crossover systems[1] mostly of iron(II) have been studied by a number of researchers over the past decades both in solution[2] as well as in the solid state.[3,4] Of particular interest for the current paper is that even in low-spin (LS) compounds with a $^1A_1(t_{2g}^6)$ ground state the $^5T_2(t_{2g}^4e_g^2)$ high-spin (HS) state can be populated efficiently by irradiation into a metal–ligand charge transfer (MLCT) absorption band and that at room temperature lifetimes of the HS state are typically in the hundreds of picoseconds to nanosecond region.[2] In contrast, the relaxation from the initially excited ^{1}MLCT state to the HS state via the ^{3}MLCT state generally takes substantially less than 1 ps.[5] In the complex $[Fe(bpy)_3]^{2+}$ for example, Cannizzo et al.[6] determined intersystem crossing times of less than 50 and 130 fs for the ^{1}MLCT→^{3}MLCT and the ^{3}MLCT→HS steps, respectively, whereby the lower energy singlet and triplet ligand-field states are effectively bypassed.

TTF (tetrathiafulvalene) and its derivatives are well-known as π electron donors capable of forming stable cation radical and dication species upon oxidation.[7] As a consequence, they are good candidates to be used as donor units in donor–acceptor compounds, which are of considerable research interest because of their potential applications in sensors, optoelectronics, and molecular devices.[8−13]

TTF can be fused to an electron acceptor unit, for instance dppz (dipyrido-[3,2-*a*:2′,3′-*c*] phenazine). The latter has two low lying π^* acceptor levels, one localized on the phenazine subunit and one on the phenanthroline subunit of dppz.[14] The fusion of TTF to dppz results in a TTF-dppz ligand with two redox centers and a lowest excited state corresponding to an intraligand charge transfer (ILCT) from the TTF to the dppz moieties. This ligand was studied on its own,[8] as well as as its ruthenium(II) complexes, including the series $[Ru(bpy)_{3-x}(TTF\text{-}dppz)_x]^{2+}$, x = 1−3.[15] These complexes show interesting photophysical properties with a long-lived, non-emissive charge separated state, in which an electron from the TTF moiety of one ligand is transferred to the dppz moiety of another one upon the initial excitation into the spin-allowed metal to ligand charge transfer (MLCT) bands. The ligand on its own as well as the complexes also show luminescence from the ^{1}ILCT state, the former with a lifetime of 450 ps and a quantum efficiency of 1% in CH_2Cl_2.[8] For the latter the quantum efficiency drops to around 20% of that of the free ligand, which has been attributed to more efficient nonradiative decay as a result of the substantial red-shift upon coordination to a metal ion.[15]

The coordination of one TTF-dppz and two phenanthroline (phen) ligands to an iron(II) ion gives rise to the complex $[Fe(phen)_2(TTF\text{-}dppz)]^{2+}$. Its synthesis has been motivated by the search for new antenna systems capable of charge separation,[15,16] new photoredox switches[17] as well as the study of the properties in relation with spin-crossover phenomena. This is in line with the international research effort on both diamagnetic complexes, for instance ruthenium(II) complexes,[15,18−24] as well as on paramagnetic complexes in combination with neutral or oxidized TTF derivatives.[25−27] Among these, the first example of the observation of both spin-

Received: September 4, 2012
Published: December 18, 2012

   dx.doi.org/10.1021/ic3019277 | *Inorg. Chem.* 2013, 52, 306−312

crossover and electrical conductivity in an iron(II) compound was reported recently.[27] Herein, we describe the synthesis of the iron(II) complex shown in Scheme 1 and thoroughly examine its electrochemical and photophysical properties.

Scheme 1. $[Fe(phen)_2(TTF\text{-}dppz)]^{2+}$

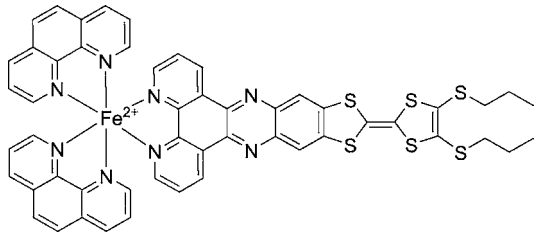

2. EXPERIMENTAL SECTION

2.1. General Procedures. Unless otherwise stated, all reagents were purchased from commercial sources and used without additional purification. 4′,5′-Bis-(propylthio)tetrathiafulvenyl[*i*]dipyrido[3,2-*a*:2′,3′-*c*]phenazine (TTF-dppz)[12] and $[Fe(phen)_2Cl_2]$[28,29] were prepared according to literature procedures. The ^{1}H NMR spectrum was obtained on a Bruker AC 300 spectrometer operating at 300.18 MHz. Chemical shifts are reported in parts per million (ppm) referenced to residual solvent protons ($CDCl_3$). The following abbreviations were used: s (singlet), d (doublet), t (triplet), m (multiplet), and br (broad). Infrared spectra were recorded on a Perkin-Elmer Spectrum One FT-IR spectrometer using KBr pellets. Elemental analyses were performed on a Carlo Erba Instruments EA 1110 Elemental Analyzer CHN. Mass spectra were recorded using a LTQ Orbitrap XL for ESI.

2.2. Synthesis of $[Fe(phen)_2(TTF\text{-}dppz)](PF_6)_2$. A solution of TTF-dppz (30 mg, 0.49 mmol) in CH_2Cl_2 (5 mL) was added to the solution of $[Fe(phen)_2Cl_2]$ (24 mg, 0.49 mmol) in ethanol (5 mL). The mixture was heated to 80 °C for 2 h. After cooling down to room temperature, aqueous potassium hexafluorophosphate was added, and the precipitate immediately formed. The dark blue powder was collected and washed with water, ethanol, and acetone. Yield: 48.9 mg (75%). ^{1}H NMR ($CDCl_3$, 300 MHz): δ = 9.53 (d, 4H), 9.22 (d, 2H), 8.52−8.48 (m, 2H), 8.14 (t, J = 6.9 Hz, 2H), 8.07 (s, 2H), 8.00−7.91 (m, 4H), 7.78−7.77 (m, 8H), 2.83 (t, J = 7.2 Hz, 4H), 1.70−1.66 (m, 4H), 1.03 (t, J = 7.2 Hz, 6H). IR (KBr): ν = 2958, 1630, 1426, 1356, 1212, 1122, 1088, 837, 722, 556 cm^{-1}. ESI-MS: m/z: 511.05, calcd for $[M-2PF_6]^{2+}$: 511.04. Anal. Calcd (%) for $C_{52}H_{38}F_{12}FeN_8P_2S_6{\cdot}2CH_3COCH_3$: C, 48.74; H, 3.53; N, 7.84. Found: C, 48.90; H, 3.19; N, 7.91.

2.3. Methods. Cyclic voltammetry was conducted on a VA-Stand 663 electrochemical analyzer. An Ag/AgCl electrode containing 2 M LiCl served as reference electrode, a glassy carbon electrode as counter electrode, and a Pt disk as working electrode. Cyclic voltammetric measurements were performed at room temperature under N_2 in CH_2Cl_2 with 0.1 M Bu_4NPF_6 as supporting electrolyte at a scan rate of 100 mV·s^{-1}.

Photophysical measurements were performed in solutions of the compounds in CH_2Cl_2 at room temperature. Spectoelectrochemical measurements were performed with a spectroelectrochemical cell designed by F. Hartl based on a standard OTTLE cell and $TBAPF_6$ as conductive salt.[30] For luminescence and transient absorption measurements, the solutions were degassed by bubbling N_2 through them for 30 min. For these experiments, the sample was changed frequently to always measure on fresh samples, as the TTF unit is known to suffer some photochemical degradation.[21] Absorption spectra were recorded on a Varian Cary 5000 UV/vis/near-IR spectrophotometer.

The femtosecond transient absorption setup has been described earlier elsewhere.[31] Briefly, the output of a Ti:Sapphire amplifier (Spitfire, Spectra Physics; 800 nm pulses of 150 fs FHWM) is split into two parts; about 5 μJ are focused into a 3 mm thick CaF_2 window that is constantly moved to generate a white light continuum that is used for probing. The remainder serves as pump and is either frequency doubled or sent into a home-built two stage noncollinear optical parametric amplifier to generate the pump pulses at 500 or 650 nm. The pump beam has an intensity of about 0.1 mJ/cm^2 at the sample, and its polarization is at magic angle with respect to the probe beam. The sample solution is located in a 1 mm quartz cell and constantly stirred by nitrogen bubbling. Its photochemical stability is verified by the steady state absorption. After the sample, the probe beam is dispersed in a spectrograph (Andor, SLR163) and imaged onto a 512 × 58 pixel back-thinned CCD (Hamamatsu S07030-09). The setup suffers from chromatic aberration distorting the shape of the spectra somewhat in the NIR spectral range.[32] The spectra are corrected for the chirp of the white light pulses by standard recipes.[33] The instrument response function (IRF) has a full width at half-maximum (FHWM) of approximately 200 fs. Because of cross-phase-modulation and the coherent signal, the spectra around time zero cannot be observed.

3. RESULTS AND DISCUSSION

3.1. Electrochemical Properties. The electrochemical properties of $[Fe(phen)_2(TTF\text{-}dppz)]^{2+}$ in CH_2Cl_2 were investigated by cyclic voltammetry (CV), as shown in Figure 1. The electrochemical data are collected in Table 1 together

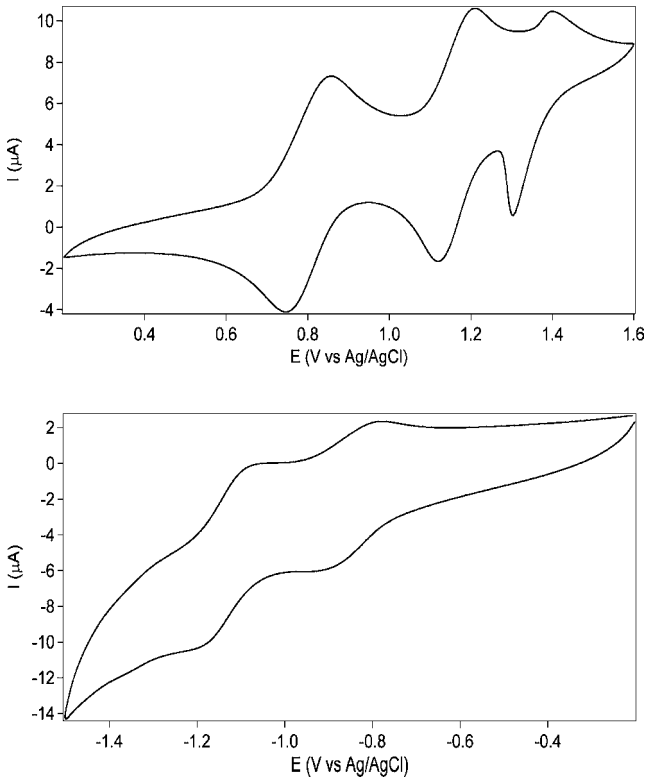

Figure 1. Cyclic voltammograms of $[Fe(phen)_2(TTF\text{-}dppz)]^{2+}$ (1×10^{-4} M) in CH_2Cl_2; 0.1 M $TBAPF_6$; on a platinum electrode at 100 mV·s^{-1}.

with those of the reference compounds TTF-dppz, $[Fe(phen)_3]^{2+}$ and $[Ru(bpy)_2(TTF\text{-}dppz)]^{2+}$ for comparison. $[Fe(phen)_2(TTF\text{-}dppz)]^{2+}$ can be oxidized in three distinct waves, at 0.80, 1.16, and 1.35 V vs Ag/AgCl, the first two being fully reversible, the third one still being quasi-reversible. The free TTF-dppz ligand has two reversible oxidation potentials at 0.73 and 1.08 V whereas $[Fe(phen)_3]^{2+}$ has an oxidation potential at 1.12 V, that is, higher than the second one of TTF-dppz. It can be deduced therefore that for $[Fe(phen)_2$(TTF-

dx.doi.org/10.1021/ic3019277 | Inorg. Chem. 2013, 52, 306−312

Table 1. Redox Potentials (V vs Ag/AgCl) of $[Fe(phen)_2(TTF\text{-}dppz)]^{2+}$ in CH_2Cl_2, Together with Those of the Reference Compounds TTF-dppz,[15] $[Fe(phen)_3]^{2+}$,[34] and $[Ru(bpy)_2(TTF\text{-}dppz)]^{2+}$[15]

	oxidation			reduction	
compound	$E_{1/2}^1$	$E_{1/2}^2$	$E_{1/2}^3$	$E_{1/2}^1$	$E_{1/2}^2$
$[Fe(phen)_3]^{2+}$[a]	1.12				
TTF-dppz	0.73	1.08		−1.17	
$[Ru(bpy)_2(TTF\text{-}dppz)]^{2+}$	0.74	1.05	1.43	−0.91	−1.35
$[Fe(phen)_2(TTF\text{-}dppz)]^{2+}$	0.80	1.16	1.35	−0.84	−1.13

[a]In MeCN, saturated calomel electrode (SCE) (for values vs Ag/AgCl, 0.04 V were added).

dppz)]$^{2+}$, the first two oxidation waves correspond to the successive oxidation of TTF-dppz, while the third one can be assigned to the $Fe^{2+/3+}$ redox couple, the previous oxidation of TTF to TTF^{2+} being responsible for the 230 mV higher value compared to $[Fe(phen)_3]^{2+}$. Similar to $[Ru(bpy)_2(TTF\text{-}dppz)]^{2+}$, two reversible reduction waves at −0.84 V and −1.13 V were observed for $[Fe(phen)_2(TTF\text{-}dppz)]^{2+}$, which are attributed to the reduction of the dppz and phen moieties, respectively.

3.2. Photophysical Properties. The absorption spectrum of $[Fe(phen)_2(TTF\text{-}dppz)]^{2+}$ in CH_2Cl_2, together with those of the reference compounds TTF-dppz, $[Fe(phen)_3]^{2+}$ and $[Fe(phen)_2(dppz)]^{2+}$ are presented in Figure 2. The broad

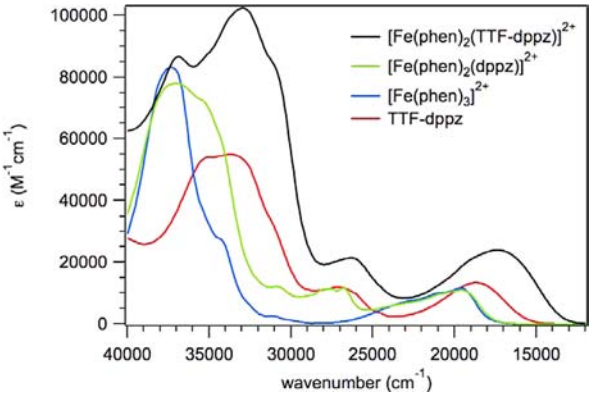

Figure 2. Absorption spectrum of $[Fe(phen)_2(TTF\text{-}dppz)]^{2+}$ (black) in comparison with those of the reference compounds $[Fe(phen)_2(dppz)]^{2+}$ (green), $[Fe(phen)_3]^{2+}$ (blue), and TTF-dppz (red), in CH_2Cl_2.

absorption band centered at 17000 cm^{-1} corresponds to the intraligand charge transfer (^{1}ILCT) transition occurring on the TTF-dppz ligand, as shown previously for the series of ruthenium(II) complexes $[Ru(bpy)_{3-x}(TTF\text{-}dppz)_x]^{2+}$, x = 1−3,[15] with the TTF subunit acting as electron donor and the dppz subunit acting as electron acceptor. The ^{1}ILCT absorption band is red-shifted by 2500 cm^{-1} with respect to the free ligand TTF-dppz, corresponding to a lowering of the energy of the lowest unoccupied molecular orbital (LUMO) located on the dppz subunit because of the coordination to the iron(II). The extinction coefficient increases from 1×10^4 to 2.4×10^4 $M^{-1}cm^{-1}$ upon coordination of one TTF-dppz and two phen ligands to iron(II). For coordination to three diimine ligands, the iron(II) center is expected to have a LS ground state.[35] By comparison with the reference complexes $[Fe(phen)_3]^{2+}$ and $[Fe(phen)_2(dppz)]^{2+}$,[36,37] the characteristic absorption bands corresponding to the ^{1}MLCT transitions of iron(II) in the LS state are expected between 18000 and 26000 cm^{-1}. Thus, the broadening of the absorption band centered at 17000 cm^{-1} and the asymmetry toward higher energy are due to the underlying presence of these ^{1}MLCT bands. This is confirmed by the difference absorption spectrum between $[Fe(phen)_2(TTF\text{-}dppz)]^{2+}$ and a mixture of Zn^{2+}/TTF-dppz (1:1)[8] shown in Figure 3, the spectrum of the zinc complex,

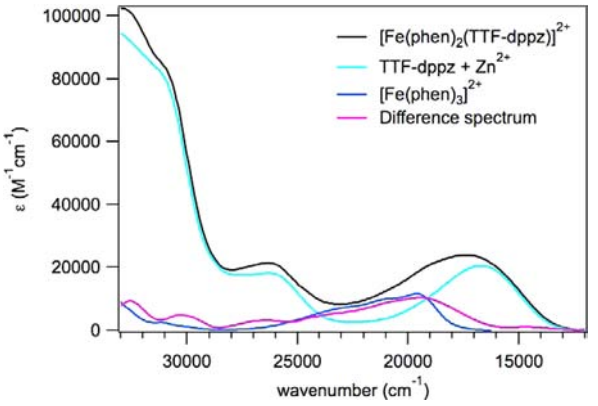

Figure 3. Absorption spectra of $[Fe(phen)_2(TTF\text{-}dppz)]^{2+}$ (black), TTF-dppz with 1 equiv of $ZnCl_2$ added (light blue) and the difference absorption spectrum (pink) in comparison with $[Fe(phen)_3]^{2+}$ (blue) in CH_2Cl_2 at room temperature. The difference spectrum is obtained by subtraction of the light blue curve from the black one. Before subtraction, the intensity of the absorption spectrum of the TTF-dppz solution with $ZnCl_2$ added was scaled to the one of $[Fe(phen)_2(TTF\text{-}dppz)]^{2+}$.

which exhibts no intense bands apart from the ^{1}ILCT band, serving as reference. This difference spectrum is indeed almost identical to the absorption spectrum of $[Fe(phen)_3]^{2+}$. Last but not least, the weakly structured absorption band centered at 26500 cm^{-1} can be assigned to the lowest energy $\pi-\pi^*$ transition located on the dppz subunit in TTF-dppz. In the UV region, the broad band with several maxima and shoulders is attributed to the $\pi-\pi^*$ transitions located on the different subunits of $[Fe(phen)_2(TTF\text{-}dppz)]^{2+}$. In contrast to $[Ru(bpy)_2(TTF\text{-}dppz)]^{2+}$,[15,24] no luminescence from either the ^{1}ILCT state of TTF-dppz or any other excited states could be detected in the limit of the sensitivity of the experimental setup.

Upon electrochemical oxidation at 0.90 V vs Ag/AgCl, that is, the first anodic peak potential of $[Fe(phen)_2(TTF\text{-}dppz)]^{2+}$ in CH_2Cl_2, the ^{1}ILCT absorption band located at 17000 cm^{-1} decreases in intensity, and two new absorption bands appear peaking at 12000 and 22300 cm^{-1}, respectively (see Figure 4). In analogy to previous studies of TTF-dppz and its complexes,[24] the new absorption bands obtained after 20 min represent the oxidation of the TTF subunit of the complex, in particular, the band in the near IR is due to the reverse ILCT transition dppz→$TTF^{\bullet+}$. This confirms the expected oxidation of the TTF unit to the $TTF^{\bullet+}$ radical in the first oxidation wave of the CV (Figure 1). Furthermore, this oxidation is fully reversible electrochemically also on a long time scale (see spectrum after subsequent reduction at 0.60 V for approximately 2 min included in Figure 4).

To arrive at a better understanding of the photophysical behavior of the iron(II) complex, transient absorption spectra were recorded on different time scales using different excitation wavelengths. Figure 5a shows the transient absorption spectra

dx.doi.org/10.1021/ic3019277 | Inorg. Chem. 2013, 52, 306−312

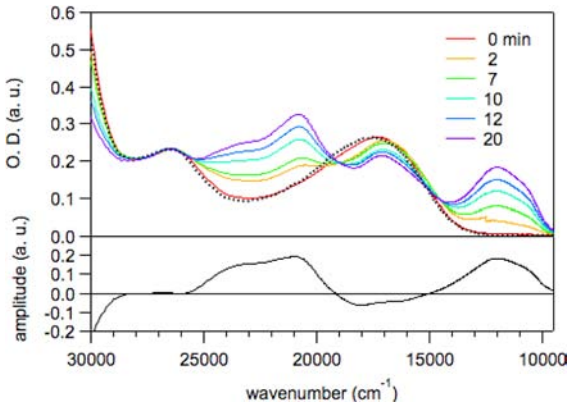

Figure 4. Absorption spectra during spectroelectrochemical oxidation of $[Fe(phen)_2(TTF\text{-}dppz)]^{2+}$ in CH_2Cl_2, at room temperature, E = 0.90 V vs Ag/AgCl in comparison with difference spectrum (black) and reversibility spectrum obtained after reduction at E = 0.60 V (dotted line).

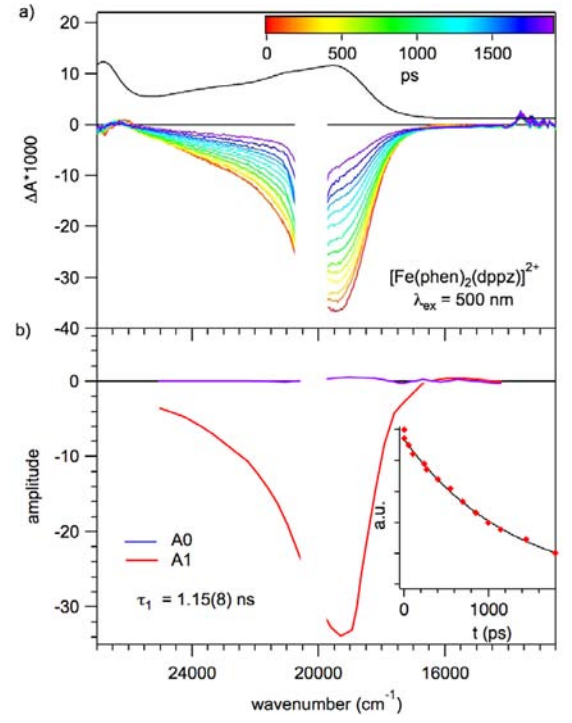

Figure 5. (a) Transient absorption spectra measured at different time delays after 500 nm excitation of $[Fe(phen)_2(dppz)]^{2+}$ in CH_2Cl_2, in comparison with its steady state absorption spectrum (black line). (b) Decay-associated spectra obtained from global analysis using $A(t) = A_0 + A_1 \exp(-t/\tau_1)$; Inset: time profile at 19000 cm^{-1} (exp: red diamonds; single exponential fit: black line. In panels (a) and (b), the spectral region around the laser wavelength is cut.

of the reference compound $[Fe(phen)_2(dppz)]^{2+}$ on the picosecond time scale upon excitation at 500 nm (20000 cm^{-1}), that is, into the Fe(II)→phen ^{1}MLCT absorption band. The transient signal essentially consists of a bleaching of the ^{1}MLCT band with the maximum at 20500 cm^{-1}. According to the global fit shown in Figure 5b, it decays monoexponentially with a lifetime of 1.15(8) ns corresponding typically to the HS→LS relaxation.[2,36] As there is no indication of an intermediate state in the transient signal, the light-induced population of the HS state via the corresponding ^{3}MLCT state occurs within the IRF in agreement with the results on $[Fe(bpy)_3]^{2+}$.[6,10]

Figure 6a shows the transient absorption spectra of $[Fe(phen)_2(TTF\text{-}dppz)]^{2+}$ also on the picosecond time scale

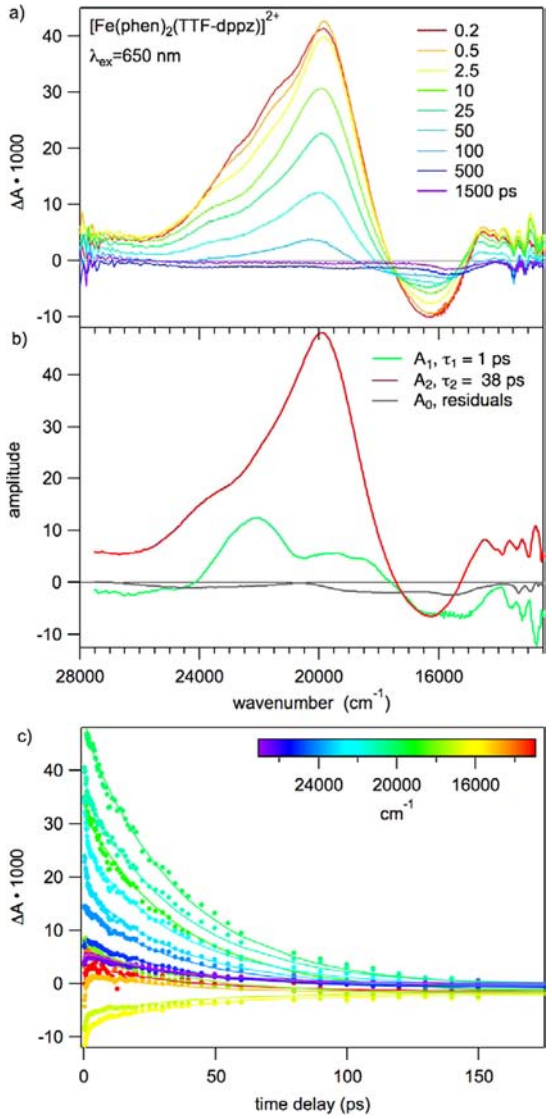

Figure 6. (a) Transient absorption spectra recorded at different time delays after excitation at 650 nm (into the ^{1}ILCT band) of $[Fe(phen)_2(TTF\text{-}dppz)]^{2+}$ in CH_2Cl_2. (b) Decay-associated spectra from global analysis of the transient spectra using a biexponential function $A(t) = A_0 + A_1 \exp(-t/\tau_1) + A_2 \exp(-t/\tau_2)$. (c) Time profiles at selected energies according to the color scheme in the inset.

upon excitation at 650 nm (15400 cm^{-1}), that is, into the ^{1}ILCT absorption band. The transient signal has a biexponential decay with $\tau_1 \approx 1$ ps and τ_2 = 38(4) ps according to the result of the global fit shown in Figures 6b and c. The initial dynamics on the time scale of 1 ps most likely reflect solvent dynamics as well as vibrational relaxation. The subsequent transient spectrum of the $[Fe(phen)_2(TTF\text{-}dppz)]^{2+}$ complex with its prominent absorption band at 20000 cm^{-1} is identical to the one of a similar ruthenium complex,[38] in which it has been attributed to the absorption of the ^{1}ILCT state itself. Complete electron transfer and formation of a radical species with $TTF^{\bullet+}$ is not likely as,

dx.doi.org/10.1021/ic3019277 | Inorg. Chem. 2013, 52, 306−312

according to the results from spectro-electrochemistry and transient absorption in an analogous ruthenium complex,[15,20c] this would result in transient absorptions at 22000 and 12000 cm^{-1} of similar intensities. However, the latter band could be obscured, as the transient absorption spectra below 14000 cm^{-1} show some artifacts from the chromatic aberration of the setup. More importantly, given the redox potential difference between the first oxidation and the first reduction of the title complex of 1.64 V (13200 cm^{-1}), the driving force for the creation of such a charge separated state with an electron residing on one of the phenanthroline ligands starting from the ^{1}ILCT is close to zero. Thus we may conclude that upon irradiation into the ^{1}ILCT transition, this state decays to the ground state in a predominantly radiationless process with a lifetime of approximately 38 ps. This also is in line with the absence of any luminescence from the ^{1}ILCT state within the sensitivity of the fluorimeter toward the NIR.

Figure 7a shows transient absorption spectra of $[Fe(phen)_2(TTF\text{-}dppz)]^{2+}$ in CH_2Cl_2 on the picosecond time scale with an excitation wavelength of 400 nm (25000 cm^{-1}), that is, with irradiation into the high-energy wing of the ^{1}MLCT transitions as well as other higher energy transitions, in particular also of the TTF-dppz moiety. In these spectra, the time evolution is clearly not single exponential. A satisfactory global fit requires a sum of four exponential functions (Figures 7b and c). As no species with $\tau > 4$ ns were detected using a standard nanosecond transient absorption setup, full ground state recovery was assumed for this fit. Initially, the transient absorption spectrum is very similar to the one observed after 650 nm excitation and shows the same relaxation associated with a time constant of $\tau_1 \approx 1.3$ ps attributed to vibrational relaxation and possibly additional ultrafast processes (see below). As time evolves, the strong transient absorption band centered at 20000 cm^{-1} decays with $\tau_2 = 35$ ps. Within experimental accuracy this is equal to the decay time for irradiation directly into the ^{1}ILCT transition. This component may therefore be assigned to the decay of the ^{1}ILCT state, being fed via fast internal conversion from the initial excitation of a higher lying state of the TTF-dppz moiety. The amplitude spectrum of the longest time constant, $\tau_4 \approx 1.46$ ns, in the fit to the sum of four exponentials with the minimum at 20500 cm^{-1} is typical for the bleaching of the ^{1}MLCT band also observed for the excitation of the $[Fe(phen)_2(dppz)]^{2+}$ reference compound. The corresponding relaxation time is likewise close to the relaxation time observed for the reference complex and is again typical for the HS→LS relaxation of iron(II) LS complexes following the ultrafast, light-induced population of the HS state via the ^{3}MLCT state.[10] Interestingly, there is an additional relaxation process with an intermediate time constant, $\tau_3 = 285$ ps, observed neither upon irradiation into the ^{1}MLCT band of the reference compound nor upon irradiation into the ^{1}ILCT band of $[Fe(phen)_2(TTF\text{-}dppz)]^{2+}$. The corresponding amplitude spectrum has a fairly strong absorption at slightly lower energy than the strong absorption typical for the excited state absorption from the ^{1}ILCT state and a bleaching at the energy of the absorption maximum of the TTF-dppz ^{1}ILCT band at 18000 cm^{-1}. It also shows a weak rise in absorption below 16000 cm^{-1}. The key question is, what is the nature of the corresponding transient state and how is it populated? The fact that this component of the transient signal shows clear bleaching at the maximum of the ^{1}ILCT transition indicates that it must be connected in some way with the TTF-dppz ligand. As mentioned above, irradiation at 400 nm excites

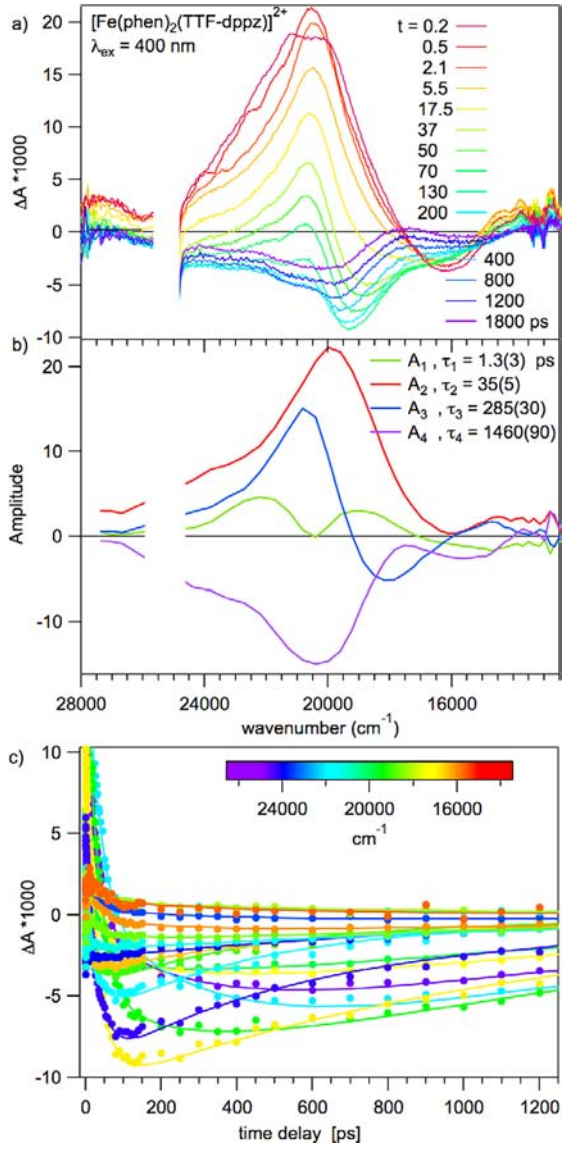

Figure 7. (a) Transient absorption spectra recorded at different time delays upon excitation at 400 nm (into the ^{1}MLCT band) of $[Fe(phen)_2(TTF\text{-}dppz)]^{2+}$ in CH_2Cl_2. (b) Decay-associated spectra obtained from a global analysis of the transient spectra using the function $\Delta A(t) = A_1 \exp(-t/\tau_1) + A_2 \exp(-t/\tau_2) + A_3 \exp(-t/\tau_3) + A_4 \exp(-t/\tau_4)$. (c) Time profiles at selected energies, experimental (●), global fit (solid line).

both ^{1}MLCT states and higher lying states of the TTF-dppz moiety. Irradiation into the ^{1}MLCT transitions may result in charge transfer either to the phenanthroline ligands or to the dppz part of the TTF-dppz with similar probabilities. For both, the first relaxation step will be ultrafast intersystem crossing to the corresponding ^{3}MLCT state. For charge transfer to the dppz moiety of the TTF-dppz ligand, the next step could be internal conversion to the ^{3}ILCT state, but a second ultrafast intersystem crossing process to the iron(II) HS state is more likely.[5,6] Similarly, for charge transfer to the phenanthroline ligands, ultrafast intersystem crossing to the HS state is bound to play a role. However, in this MLCT state the iron center is formally in a 3+ oxidation state and thus becomes a good electron acceptor. With the corresponding electron sitting on phenathroline, fast excited state electron transfer from the TTF moiety across the conjugated dppz bridge to the formal

dx.doi.org/10.1021/ic3019277 | Inorg. Chem. 2013, 52, 306−312

iron(III) center could competitively lead to a charge-separated state, similar to the one observed for the analogous ruthenium complex.[15] In contrast to the ruthenium complex, this state is not long-lived because of the low-lying metal-centered e_g orbitals which provide a ladder of low-energy dd states for efficient nonradiative relaxation to the iron(II) HS state or the ground state. The transient component with τ_3 = 285 ps may thus tentatively be ascribed to the lifetime of such a charge separated state with a $TTF^{\bullet+}$ radical and an electron on one of the phenanthroline ligands.

4. CONCLUSIONS

The title complex, $[Fe(phen)_2(TTF\text{-}dppz)]^{2+}$ with the iron(II) center in the LS state, was engineered to study light-induced electron transfer, as well as spin-crossover phenomena. Time-resolved spectroscopy on the picosecond time scale led to the identification of the various processes summarized in Figure 8.

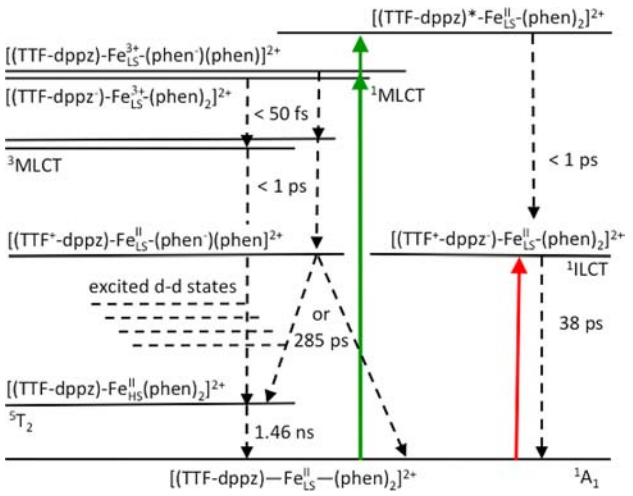

Figure 8. Scheme of the ground and excited states of $[Fe(phen)_2(TTF\text{-}dppz)]^{2+}$ and the dominant nonradiative relaxation pathways for excitation into the different absorption bands.

The first excited state of the complex is the corresponding low-energy HS state of iron(II) with a lifetime of 1.46 ns populated via ultrafast relaxation from the initially excited ^{1}MLCT states upon irradiation at 400 nm. The HS state is too low in energy to induce any further processes except for the relaxation back to the ground state, the 1.46 ns thus correspond exclusively to the HS→LS relaxation with a relaxation rate constant of 7×10^8 s^{-1} at room temperature in solution.

The ^{1}ILCT state, which can be populated by direct irradiation or via irradiation into higher lying TTF-dppz centered states and internal conversion, has a lifetime of around 38 ps. This is much shorter than the 450 ps found for the ^{1}ILCT lifetime of the free ligand in CH_2Cl_2,[8] but only sligthly shorter than the one found for the analogous Ru(II) complex, for which, in the absence of any lower lying excited states, the ^{1}ILCT lifetime was estimated to be around 100 ps.[15] According to the transient absorption spectra presented above, the ^{1}ILCT state decays predominantly directly to the ground state. Indeed there is no plausible mechanism for efficient decay of the ^{1}ILCT state via the iron(II) HS state, considering that for the ΔS = 2 intersystem crossing process with the wave function of the initial state being localized on the periphery of the TTF-dppz ligand and the final wave function being metal centered, the electronic interaction must be small.

What about the population of a long-lived charge separated state as observed in the Ru(II) analogue, in which such a state with a $TTF^{\bullet+}$ radical and the electron on the auxiliary ligand was observed with a lifetime of 2.45 μs?[15] In the present system the population of such a state upon excitation of the MLCT transition to the phenanthroline ligands is in direct competition with the ultrafast relaxation to the iron(II) HS state. The latter occurs within substantially less than 1 ps,[6] that is, close to or within the IRF of the experimental setup. Despite this there is a component in the transient spectrum with some of the characteristics of such a charge-separated state, albeit with a much shorter lifetime than for the analogous ruthenium complex. This can be explained by the low-lying dd states of the iron(II) complex. However, the complexity of the processes and number of states involved does not allow a more definite assignment of the intermediate state with the time constant of 285 ps, nor of the exact pathway leading to its population or the pathways of its decay. Attribution of this state to a ^{3}ILCT state cannot be entirely ruled out.

Further systems of potential interest to be studied in view of light-induced intramolecular electron transfer comprise complexes of cobalt(II) and cobalt(III) with the TTF-dppz ligand. In particular for complexes of cobalt(III), light-induced electron transfer processes and charge separated states are to be expected in analogy to the intensively studied catecholate systems.[38]

AUTHOR INFORMATION

Corresponding Author

*E-mail: andreas.hauser@unige.ch (A.H.), shi-xia.liu@iac.unibe.ch (S.-X.L.).

Notes

The authors declare no competing financial interest.

ACKNOWLEDGMENTS

This work was supported by the Swiss National Science Foundation (Grant Nos. 200020-125175 and 200020-130266).

REFERENCES

(1) *Spin Crossover in Transition Metal Compounds I–III; Topics in Current Chemistry*; Gütlich, P., Goodwin, H. A., Eds.; Springer: Berlin, Germany, 2004; Vols. *233–235*.

(2) Brady, C.; McGarvey, J. J.; McCusker, J. K.; Toftlund, H.; Hendrickson, D. N. *Top. Curr. Chem.* **2004**, *235*, 288.

(3) (a) Decurtins, S.; Gütlich, P.; Hasselbach, K. M.; Hauser, A.; Spiering, H. *Inorg. Chem.* **1985**, *24*, 2174. (b) Gütlich, P.; Hauser, A.; Spiering, H. *Angew. Chem., Int. Ed. Eng.* **1994**, *33*, 2024. (c) Hauser, A. *Top. Curr. Chem.* **2004**, *234*, 155.

(4) Létard, J. F. *J. Mater. Chem* **2006**, *16*, 2550.

(5) (a) Wolf, M. M. N.; Gross, R.; Schumann, C.; Wolny, J. A.; Schünemann, V.; Dossing, A.; Paulsen, H.; McGarvey, J. J.; Diller, R. *Phys. Chem. Chem. Phys.* **2008**, *10*, 4264. (c) Smeigh, A. L.; Creeelman, M.; Mathies, R. A.; McCusker, J. K. *J. Am. Chem. Soc.* **2008**, *130*, 14105.

(6) (a) Consani, C.; Premont-Schwarz, M.; ElNahhas, A.; Bressler, C.; van Mourik, F.; Cannizzo, A.; Chergui, M. *Angew. Chem., Int. Ed.* **2009**, *48*, 7184. (b) Bressler, C.; Milne, C.; Pham, V.-T.; ElNahhas, A.; van der Veen, R. M.; Gawelda, W.; Johnson, S.; Beaud, P.; Grolimund, D.; Kaiser, M.; Borca, C. N.; Ingold, G.; Abela, R.; Chergui, M. *Science* **2009**, *323*, 489. (c) Cannizzo, A.; Milne, C. J.; Consani, C.; Gawelda, W.; Bressler, C.; van Mourik, F.; Chergui, M. *Coord. Chem. Rev.* **2010**, *254*, 2677.

(7) (a) Jorgensen, T.; Hansen, T. K.; Becher, J. *Chem. Soc. Rev.* **1994**, *23*, 41. (b) Segura, J. L.; Martin, N. *Angew. Chem., Int. Ed.* **2001**, *40*, 1372. (c) Canevet, D.; Sallé, M.; Zhang, G.; Zhang, D.; Zhu, D. *Chem. Commun.* **2009**, 2245.
(8) Jia, C. Y.; Liu, S.-X.; Tanner, C.; Leiggener, C.; Neels, A.; Sanguinet, L.; Levillain, E.; Leutwyler, S.; Hauser, A.; Decurtins, S. *Chem.—Eur. J.* **2007**, *13*, 3804.
(9) (a) Dumur, F.; Gautier, N.; Gallego-Planas, N.; Sahin, Y.; Levillain, E.; Mercier, N.; Hudhomme, P.; Masino, M.; Girlando, A.; Lloveras, V.; Vidal-Gancedo, J.; Veciana, J.; Rovira, C. *J. Org. Chem.* **2004**, *69*, 2164. (b) Jia, C. Y.; Liu, S.-X.; Tanner, C.; Leiggener, C.; Sanguinet, L.; Levillain, E.; Leutwyler, S.; Hauser, A.; Decurtins, S. *Chem. Commun.* **2006**, 1878.
(10) Fuks-Janczarek, I.; Luc, J.; Sahraoui, B.; Dumur, F.; Hudhomme, P.; Berdowski, J.; Kityk, I. V. *J. Phys. Chem. B* **2005**, *109*, 10179.
(11) Loosli, C.; Jia, C. Y.; Liu, S.-X.; Haas, M.; Dias, M.; Levillain, E.; Neels, A.; Labat, G.; Hauser, A.; Decurtins, S. *J. Org. Chem.* **2005**, *70*, 4988.
(12) Perepichka, D. F.; Bryce, M. R.; Pearson, C.; Petty, M. C.; McInnes, E. J.; Zhao, J. P. *Angew. Chem., Int. Ed.* **2003**, *42*, 4636.
(13) Wu, J.; Liu, S.-X.; Neels, A.; Derf, F. L.; Sallé, M.; Decurtins, S. *Tetrahedron* **2007**, *63*, 11282.
(14) Lopez, R.; Leiva, A. M.; Zuloaga, F.; Loeb, B.; Norambuena, E.; Omberg, K. M.; Schoonover, J. R.; Striplin, D.; Devenney, M.; Meyer, T. J. *Inorg. Chem.* **1999**, *38*, 2924.
(15) Goze, C.; Leiggener, C.; Liu, S.-X.; Sanguinet, L.; Levillain, E.; Hauser, A.; Decurtins, S. *ChemPhysChem* **2007**, *8*, 1504.
(16) Wu, H.; Zhang, D. Q.; Su, L.; Ohkubo, K.; Zhang, C. X.; Yin, S. W.; Mao, L. Q.; Shuai, Z. G.; Fukuzumi, S.; Zhu, D. B. *J. Am. Chem. Soc.* **2007**, *129*, 6839.
(17) Fang, C. J.; Zhu, Z.; Sun, W.; Xu, C. H.; Yan, C. H. *New J. Chem.* **2007**, *31*, 580.
(18) Campagna, S.; Serroni, S.; Puntoriero, F.; Loiseau, F.; De Cola, L.; Kleverlaan, C. L.; Becher, J.; Sorensen, A. P.; Hascoat, P.; Thorup, N. *Chem.—Eur. J.* **2002**, *8*, 4461.
(19) Bryce, M. R. *Adv. Mater.* **1999**, *11*, 11.
(20) (a) Goze, C.; Liu, S.-X.; Leiggener, C.; Sanguinet, L.; Levillain, E.; Hauser, A.; Decurtins, S. *Tetrahedron* **2008**, *64*, 1345. (b) Goze, C.; Dupont, N.; Beitler, E.; Leiggener, C.; Jia, H.; Monbaron, P.; Liu, S.-X.; Neels, A.; Hauser, A.; Decurtins, S. *Inorg. Chem.* **2008**, *47*, 11010. (c) Dupont, N.; Ran, Y.-F.; Jia, H.-P.; Grilj, J.; Ding, J.; Liu, S.-X.; Decurtins, S.; Hauser, A. *Inorg. Chem.* **2011**, *50*, 3295.
(21) Keniley, L. K.; Ray, L.; Kovnir, K.; Dellinger, L. A.; Hoyt, J. M.; Shatruk, M. *Inorg. Chem.* **2010**, *49*, 1307.
(22) Vacher, A.; Barriere, F.; Roisnel, T.; Lorcy, D. *Chem. Commun.* **2009**, 7200.
(23) Pointillart, F.; Le Gal, Y.; Golhen, S.; Cador, O.; Ouahab, L. *Inorg. Chem.* **2008**, *47*, 9730.
(24) Leiggener, C.; Dupont, N.; Liu, S.-X.; Goze, C.; Decurtins, S.; Beitler, E.; Hauser, A. *Chimia* **2007**, *61*, 621.
(25) (a) Hervé, K.; Liu, S.-X.; Cador, O.; Golhen, S.; Le Gal, Y.; Bousseksou, A.; Stoeckli-Evans, H.; Decurtins, S.; Ouahab, L. *Eur. J. Inorg. Chem.* **2006**, 3498. (b) Smucker, B. W.; Dunbar, K. R. *J. Chem. Soc., Dalton Trans.* **2000**, 1309. (c) Avarvari, N.; Martin, D.; Fourmigué, M. *J. Organomet. Chem.* **2002**, *643*−*644*, 292. (d) Ichikawa, S.; Kimura, S.; Takahashi, K.; Mori, H.; Yoshida, G.; Manabe, Y.; Matsuda, M.; Tajima, H.; Yamaura, J. *Inorg. Chem.* **2008**, *47*, 4140. (e) Liu, S.-X.; Ambrus, C.; Dolder, S.; Neels, A.; Decurtins, S. *Inorg. Chem.* **2006**, *45*, 9622. (f) Pointillart, F.; Cauchy, T.; Le Gai, Y.; Golhen, S.; Cador, O.; Ouahab, L. *Inorg. Chem.* **2010**, *49*, 1947. (g) Wu, J.-C.; Liu, S.-X.; Keene, T. D.; Neels, A.; Mereacre, V.; Powell, A. K.; Decurtins, S. *Inorg. Chem.* **2008**, *47*, 3452.
(26) (a) Fu, X. C.; Li, M. T.; Wang, C. G. *Acta Crystallogr., Sect. E: Struct. Rep. Online* **2005**, *61*, M1221. (b) Liu, S.-X.; Dolder, S.; Rusanov, E. B.; Stoeckli-Evans, H.; Decurtins, S. *C. R. Chim.* **2003**, *6*, 657. (c) Delahaye, S.; Loosli, C.; Liu, S.-X.; Decurtins, S.; Labat, G.; Neels, A.; Loosli, A.; Ward, T. R.; Hauser, A. *Adv. Funct. Mater.* **2006**, *16*, 286. (d) Ran, Y.-F.; Liu, S.-X.; Sereda, O.; Neels, A.; Decurtins, S. *Dalton Trans.* **2011**, *40*, 8193. (e) Ran, Y.-F.; Steinmann, M.; Sigrist, M.; Liu, S.-X.; Hauser, J.; Decurtins, S. *C. R. Chim.* **2012**, *15*, 838. (f) Shatruk, M.; Lipika, R. *Dalton Trans.* **2010**, *39*, 11105. (g) Lorcy, D.; Bellac, N.; Fourmigué, M.; Avarvari, N. *Coord. Chem. Rev.* **2009**, *253*, 1398.
(27) Nihei, M.; Takahashi, N.; Nishikawa, H.; Oshio, H. *Dalton Trans.* **2011**, *40*, 2154.
(28) Fu, X. C.; Li, M. T.; Wang, C. G. *Acta Crystallogr., Sect E* **2005**, *61*, m1221.
(29) Madeja, K.; Wilke, W.; Schmidt, S. *Z. Anorg. Allg. Chem.* **1966**, *346*, 306.
(30) Krejčík, M.; Daněk, M.; Hartl, F. *J. Electroanal. Chem.* **1991**, 317.
(31) Banerji, N.; Duvanel, G.; Perez-Velasco, A.; Maity, S.; Sakai, N.; Matile, S.; Vauthey, E. *J. Phys. Chem. A* **2009**, *113*, 8202.
(32) Yanshole, V.; Sherin, P. S.; Gritsan, N. P.; Snytnikova, O. A.; Mamatyuk, V. I.; Grilj, J.; Vauthey, E.; Sagdeev, R. Z.; Tsentalovich, Y. P. *Phys. Chem. Chem. Phys.* **2010**, *12*, 9502.
(33) Yamaguchi, S.; Hamaguchi, H. O. *Appl. Spectrosc.* **1995**, *49*, 1513.
(34) Richert, S. A.; Tsang, P. K. S.; Sawyer, D. T. *Inorg. Chem.* **1989**, *28*, 2471.
(35) Hauser, A.; Jeftic, J.; Romstedt, H.; Hinek, R.; Spiering, H. *Coord. Chem. Rev.* **1999**, *471*, 190.
(36) Braterman, P. S.; Song, J. I.; Peacock, R. D. *Inorg. Chem.* **1992**, *31*, 555.
(37) Mudasir; Wijaya, K.; Wahyuni, E. T.; Inoue, H.; Yoshioka, N. *Spectrochim. Acta, Part A* **2007**, *66*, 163.
(38) (a) Beni, A.; Dei, A.; Laschi, S.; Rizzitano, M.; Sorace, L. *Chem.—Eur. J.* **2008**, *14*, 1804. (b) Dapporto, P.; Dei, A.; Poneti, G.; Sorace, L. *Chem.—Eur. J.* **2008**, *14*, 10915.